Particle mass transport in impact electrochemistry

Serge G Lemay, Christophe Renault, Jeffrey E Dick

Particle mass transport in impact electrochemistry

Serge G. Lemay*, Christophe Renault, Jeffrey E. Dick

Faculty of Science and Technology and MESA+ Institute for Nanotechnology, University of Twente, PO Box 217, 7500 AE Enschede, The Netherlands

Christophe Renault,

Department of Chemistry, Purdue University, West Lafayette, IN, 47906, USA

Jeffrey E. Dick,

Department of Chemistry, Purdue University, West Lafayette, IN, 47906, USA
Elmore Family School of Electrical and Computer Engineering, Purdue University, West Lafayette, IN, 47906, USA

*s.g.lemay@utwente.nl

Abstract

Impact electrochemistry is a set of methods in which individual micro- or nanoscale particles are detected and analyzed at a miniaturized electrode. Quantitative interpretation of the results, in particular the determination of ultralow concentrations, relies heavily on modeling the mass transport of the particles being analyzed. This is particularly subtle since, due to favorable scaling with increasing particle size, migration and convection play a disproportionate role in the transport of such particles compared to that of small molecules. Here we summarize the main governing principles in electrochemically-driven particle transport. We particularly emphasize the difference between particle electrophoresis and small-ion migration, which has led to inaccuracies in the recent literature.

Keywords

Single entity electrochemistry; particle impact electrochemistry; mass transport; migration; electroosmosis, tether forces.

Introduction

Particle-impact electrochemistry is a set of stochastic methods in which collisions of single micro- and nanoparticles with a (miniaturized) electrode generate discrete (most commonly amperometric) signals. This approach represents a branch of single-entity electrochemistry [1] and offers a promising route towards digital sensing [2]. In the most widely studied variants, signals can result from the influence that the particle has on the mass transport of a redox mediator (current blockade [3, 4]), the oxidation or reduction of the particle material itself (direct faradaic impact or stripping [5]), or the catalytic response of the particle (mediated faradaic impact [6]). The rate, size and shape of the discrete signals encode information about the concentration, charge, shape, composition and reactivity of the particles. Extracting this information, however, requires detailed understanding of the processes at work. Because of their relatively large size, mass transport of particles is far more influenced by migration and convection than that of the typically-used electrochemical molecular species, which are commonly controlled by diffusion. Perturbations introduced by the electrochemical process are sufficient to significantly influence transport, which means that great care must be exerted in extracting quantitative information from particle impact measurements. With this in mind, here we summarize the main concepts that govern the mass transport of particles in impact electrochemistry.

Diffusion

The diffusion of nano- and microparticles follows the same principles as the diffusion of molecular species. The rate of diffusive transport of particles to a shrouded disk electrode with radius r_e, for example, is given by the classic result [7]

$$j_{\mathrm{dif}} = 4D_p n_p r_e \tag{1}$$

where D_p and n_p are the diffusion coefficient and the number density of the particles, respectively, and r_e is the electrode radius. According to the Einstein relation, the diffusion coefficient of a particle (neglecting near-wall effects for simplicity [8]) is given by

$$D_p = \frac{kT}{\xi_p} = \frac{kT}{6\pi\eta r_p} \tag{2}$$

where *kT* is the thermal energy and ξ_p is the Stokes drag coefficient arising from interactions with the fluid. The middle expression is general while the last expression corresponds to the specific case of a spherical particle of radius r_p for which $\xi_p = 6\pi\eta r_p$ with η the fluid viscosity. Eq 2 indicates that D_p decreases with increasing particle size, leading to decreased diffusion for larger particles.

Migration

A particle in an external electric field $\boldsymbol{E}$ moves with velocity $\boldsymbol{v}_p = \mu_p \boldsymbol{E}$, where μ_p is its electrophoretic mobility. In the majority of impact electrochemistry experiments, the condition $r_p \gg \lambda_D$, where λ_D is the Debye screening length, is satisfied. In this case μ_p obeys the Helmholtz-Smoluchowski equation [9],

$$\mu_p = \frac{\epsilon\zeta_p}{\eta} = \frac{\sigma_p\lambda_D}{\eta} \qquad (r_p \gg \lambda_D) \tag{3}$$

Here ϵ is the permittivity of the solution and ζ_p is the zeta potential of the particle. ζ_p is related to the particle surface charge density, σ_p, as well as the electrolyte composition. The middle term is general whereas the one on the right corresponds to the explicit form for ζ_p in the Debye-Hückel approximation. Notably, eq 3 indicates that μ_p is generally independent of the particle shape or size.

Colloidally stable particles typically have ζ_p on the order of 10's of millivolts. Together with eq 3, this indicates that, contrary to the diffusion coefficient, different types and sizes of particles generally have electrophoretic mobilities of the same order of magnitude (somewhat lower zeta potentials have however been studied by impact electrochemistry in emulsions, for example [10]). Consequently, it is quite common for transport of small molecules (large D_p) to be dominated by diffusion while transport of larger particles (small D_p) to be dominated by migration.

Faradaic processes at an electrode generate electric fields that lead to uncompensated ohmic potential drops. This behavior is commonly suppressed through a large excess of supporting electrolyte. For example, consider the electric field generated during a current blockade experiment by the steady-state diffusion-limited one-electron oxidation of a neutral redox mediator at a hemispherical electrode of radius r_e. The electric field is then [11, 12]

$$E(r) = \frac{kT}{2e}\frac{r_e}{\gamma r^2} \quad (\gamma > 1) \tag{4}$$

where γ is the (monovalent) supporting electrolyte ratio and r is the distance from the center of the electrode. Increasing γ decreases the magnitude of $E(r)$, but a residual field always remains. The corresponding migration flux of particles is

$$j_{\mathrm{mig}} = \frac{kT}{e}\frac{\pi\mu_p r_e}{\gamma} \quad (\gamma > 1) \tag{5}$$

This formulation for the migration flux is less general than one based on the faradaic current and ion mobilities [3], as it applies to a specific solution composition, but it is introduced here to show explicitly the role of the supporting electrolyte.

The diffusive and migration fluxes of particles to the electrode as given by eq 1 and eq 5 are plotted in **Figure 1** with respect to r_p for typical parameters. We can see that particle migration dominates over diffusion under most circumstances. This is true for low γ values, as might be expected, but also at a 'sufficiently large' support ratio of $\gamma = 100$ for particles with $r_p \gtrsim 50$ nm. (This initially came as a surprise when we performed the first current blockade experiments and observed many more events than had been estimated based on pure diffusion [3]).

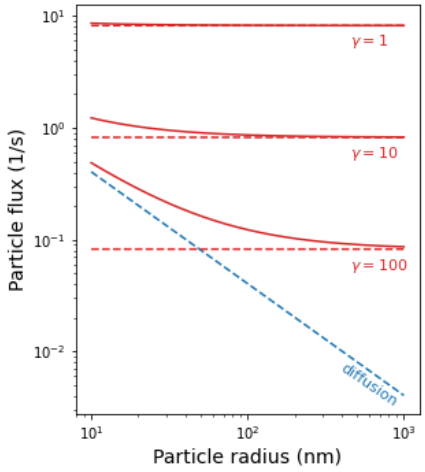

Figure 1. Impact rate versus particle radius for pure diffusion (dashed blue line), pure migration (dashed red lines, for different supporting electrolyte ratios γ) and the sum of the two components (solid red lines). Based on $T = 293$ K, $r_e = 5$ µm, $\eta = 10^{-3}$ kg/sm, $\epsilon_r = 78$, and $\zeta = -50$ mV.

The plots in Figure 1 differ from those published in recent works [13, 14] in that they exhibit a size-independent migration flux. The origin of this discrepancy is that these recent works employ the Hückel-Onsager law [9] instead of eq 3 for the electrophoretic mobility,

$$\mu_p = \frac{2}{3}\frac{\epsilon\zeta_p}{\eta} = \frac{2}{3}\frac{\sigma_p r_p}{\eta} \qquad (r_p \ll \lambda_D) \tag{6}$$

This expression exhibits a dependence on r_p for a fixed σ_p, in contrast to the Helmholtz-Smoluchowski law (eq 3). More explicitly, apart from the numerical factor of 2/3, the two equations differ in that the factor λ_D in eq 3 (a property of the solution) is replaced by a factor r_p in eq 6 (a property of the particle). The physical origin of this difference is that when $r_p \ll \lambda_D$, the forces acting on the particle are the bare electrostatic force acting on its total charge and the opposing Stokes drag. The shear force leading to drag is set by the size of the particle r_p, as described in eq 2. When $r_p \gg \lambda_D$, on the other hand, the electrostatic force, which also acts with an equal but opposite magnitude on the thin electrical double layer around the particle, instead causes the fluid to be sheared on a length scale λ_D. This causes the drag to be larger by a factor r_p/λ_D and the mobility to be smaller by a factor λ_D/r_p compared to the small-particle case (ironically this is often described as the particle having a smaller "effective charge", but the culprit is hydrodynamics). Eq 6 is appropriate to describe the migration of small ions [7], but it is rarely applicable for experimental situations involving larger particles. In the majority of cases in

impact electrochemistry, eq 3 should be used instead. An alternative to eq 3 is to employ experimental values of the mobility (as was done in a recent work on bacteria, for example [15]). This is in practice completely equivalent since most zeta potentials measurement methods, such as dynamic light scattering (DLS), infer ζ_p by measuring μ_p and applying eq 3.

Other solution compositions and electrode geometries can lead to more complex forms than eq 4, but the magnitude of the electric field remains comparable. In particular, the shape of the electrode does not have much impact on the distance dependence of the electric field: far from the electrode, the field always falls off as $1/r^2$. This is because, insofar as charge neutrality holds, the electrostatic potential $\varphi(r,\theta,\varphi)$ obeys the Laplace equation, $\nabla^2\varphi = 0$, whose solution can be expanded in the form [16],

$$\varphi(r,\theta,\varphi) = \sum_{l=0}^{\infty}\sum_{m=-l}^{l}\left[A_{lm}r^{l} + B_{lm}r^{-(l+1)}\right]Y_{lm}(\theta,\varphi) \qquad (4)$$

Here $Y_{lm}(\theta,\varphi)$ are the so-called spherical harmonics while A_{lm} and B_{lm} are a set of constants that are specified by the boundary conditions. Under the common convention that $\varphi(r\to\infty) = 0$, $A_{lm} = 0$ for all l and m. Furthermore the contribution to the potential from the terms with $l > 0$ fall off faster with increasing r than the $l = 0$ term. Consequently, at large enough r (in practice a few times the electrode size) the $1/r$ term dominates this expansion. Qualitatively, the picture that emerges is that details of the shape of the electrode get washed away with increasing distance until only a simple spherically symmetric distribution (the Y_{00} term) remains. The corresponding expression for the electric field far from the electrode reduces to the universal form $E(r) = -\nabla\varphi(r,\theta,\varphi) = -B_{00}/\sqrt{4\pi}r^2$, with only the numerical value of the constant B_{00} depending on the size and geometry of the electrode. This generally applies to disks, hemispheres, bands, recessed electrodes, spheroids, and their ensembles, so long as steady state is reached. The same principle holds for diffusive transport since the diffusion equation also reduces to the Laplace equation in the steady state. This convenient property of the Laplace equation can be used to improve the accuracy of finite element calculations by matching the numerical solution to the analytical form at the boundary of a simulated hemispherical volume [3]. It also implies that the size and shape of the electrode do not affect the ratio between j_{dif} and j_{mig} as these factors affect both types of transport equally.

Electric fields arise to some level in all forms of particle impact electrochemistry measurements. In current blockade measurements, this is explicit because of the presence of a redox mediator. In the specific case of eq 5, for example, the mediator concentration enters the equation for the electric field via the support ratio, γ. But faradaic currents are also to some degree present in other types of impact electrochemistry, as they can result from background reactions or from previously landed particles at the electrode in catalytic detection experiments. Simply put, if the current at the working electrode is not precisely zero (and it only ever is transiently), then electric fields cause at least some degree of particle migration. Because larger particles are very sensitive to migration, as illustrated in Figure 1, even non-essential background reactions can potentially lead to migration-dominated mass transport. This complication is largely ignored in the literature outside current blockade impact.

We note that migration can effectively prevent particle impacts if the polarity of the electric field is such that it repels the particles instead of attracting them. As indicated by eq 1, a net oxidation reaction causes negatively charged particles to migrate towards the electrode and positive particles to be repelled. The opposite is true of a cathodic current since this leads to electric fields with the opposite polarity. For example, in a recent work on hemispherical Hg electrodes using ruthenium hexamine reduction as a mediator, amine-functionalized polystyrene particles were employed instead of bare polystyrene [14].

The discussion above has focused on the long-range transport of particles from bulk solution to an electrode. Several groups have also interrogated the fascinating internal dynamics of collision events on the ms time scale [17-21]. Detailed analysis of these results focused on diffusion and ignored migration entirely. This can be rationalized by noting that the distance traveled by a particle within a time scale τ by migration is $l_{\mathrm{mig}} = \mu_p E\tau$, while the corresponding length scale for diffusion is $l_{\mathrm{dif}} \approx \sqrt{2D\tau}$. The ratio $l_{\mathrm{dif}}/l_{\mathrm{mig}} \sim \tau^{-1/2}$ diverges at short τ, reflecting the fact that diffusion dominates at sufficiently short length and time scales.

Convection

Just as for migration, convection may play a more substantial role for particle transport than is conventionally thought of due to the low diffusivity of larger particles. Externally imposed convection can usually be assumed to be insignificant at the length scales involved in particle impact experiments, but an additional local source of convection arises from the electrochemical process itself in the form of electroosmotic flows (EOFs). In short, EOFs are generated when an electric field oriented parallel to a charged surface exerts a net force on the ions forming the electrical double layer at that surface. Just like in particle electrophoresis, the force exerted on the ions is transferred to the fluid through viscous drag, leading to flow. Earlier examples in the context of electrochemistry include micropumping generated at bimetallic electrodes [22] and in nanocapillary array membranes [23].

This scenario also arises for shrouded electrodes, albeit in a more subtle manner. A radial electric field is necessarily generated along the (charged) surface of the insulator surrounding an electrode during a faradaic process. For a disk electrode, for example, a faradaic reaction gives rise to a toroidal flow pattern, as illustrated from simulations in **Figure 2**. The speeds at which the fluid is propelled are comparable to those of electrophoretically driven particles, and can thus have a profound impact on their trajectories. This effect was recently reported for both bacterial [24] and synthetic [25] microparticles. It was further invoked to explain the changes in configuration of graphene nanoplatelets during collision events [26].

The convective behavior has important qualitative consequences. In particular, it leads to “near-miss” events in which particles migrate toward the electrode, only to be deflected by the EOF. If the deflection occurs far from the electrode (a few times r_p), the particle may not be detected at all. Interestingly, at sufficiently low supporting electrolyte ratio, electrochemically induced convection is also sufficiently pronounced to influence the transport-limited current of a neutral redox species [25].

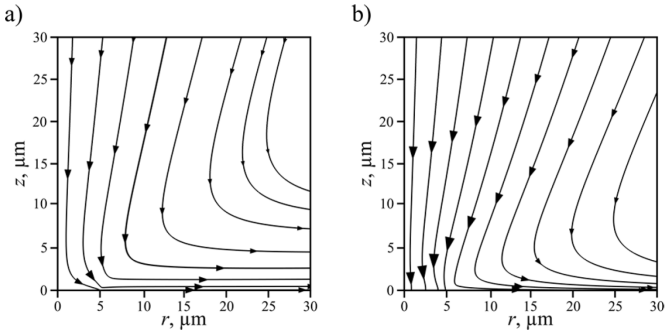

Figure 2. Simulated streamline plots for (a) solution and (b) particle velocities near a disk microelectrode during steady-state oxidation of a redox mediator (5 µm electrode radius, 2 mM redox mediator, 0.035 mM supporting electrolyte). The plots are in cylindrical coordinates and axisymmetric, with $(r, z) = (0, 0)$ corresponding to the electrode center. (a) The solution

exhibits an outward flow along the surface due to the oxidation-induced EOF. This in turn induces a downward flow of fluid above the electrode. (b) The EOF causes some particles to be deflected from the electrode. Reprinted with permission from [24]. Copyright 2020 American Chemical Society.

Electrophoretic forces on particles

A charged particle that migrates in solution under the influence of an electric field experiences no net force since the direct electrostatic force is exactly counterbalanced by viscous drag (usually from shear taking place within the electrical double layer, as discussed above). In order to hold the particle motionless in an electric field, however, an external force must be applied. This scenario can arise when a particle is held in place by a linker such as a long polymer, as illustrated in **Figure 3**. The electrophoretic force F_p acting on a tethered particle in an electric field is given by [27]

$$\boldsymbol{F}_p = \xi_p \mu_p \boldsymbol{E}$$

Combined with eq 3 and eq 4, this yields an estimate for the force on a particle near the surface of an electrode and in the presence of a redox mediator

$$F_p \approx \frac{3\pi kT\epsilon\zeta_p}{e\gamma}\frac{r_p}{r_e} \quad (r_p \ll r_e, \gamma > 1)$$

The magnitude of the force is rather modest. For example, $\gamma = 100$ and other parameters as per Figure 1, the force is 9 fN. This is barely sufficient to, e.g., deform a double-stranded DNA linker, and is negligible for typical polymers with shorter persistence lengths. The faradaic process is therefore not expected to significantly influence the tethering properties at high supporting ratios. This is in contrast to the case of polymers translocating through nanoscale pores, where the electric field is highly focused by the pore and the forces become appreciable [28]. Care must however be exerted with nanoscale electrodes or at very low supporting ratios, where more significant forces in the pN range become accessible. While this interplay of forces has not yet been explored experimentally in the context of impact electrochemistry, it is likely to become relevant as affinity-based sensors are constructed based on impact methods.

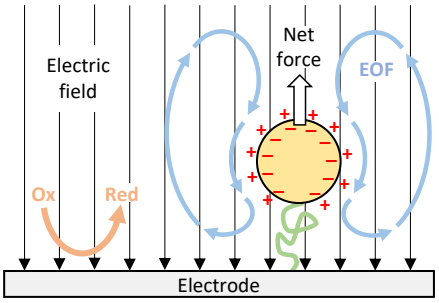

Figure 3. Schematic illustration of the interplay of forces induced by a redox reaction on a tethered particle. In this example, reduction of a redox mediator at the electrode causes an electric field oriented toward the electrode. The repulsive electric force exerted by this field on the negatively charged particle is partially cancelled by the force on the positive electrical double layer surrounding it. The latter is communicated mechanically to the particle via viscous drag from the EOF induced around the particle.

Conclusion and outlook

We have argued that electrophoretic and electroosmotic forces play a disproportionate role in determining the trajectories of micro- and nanoparticles in impact electrochemistry experiments. This is most evident in current blockade impact, where the use of a redox mediator necessarily implies the generation of electric fields and convective flows. In practice, however, background currents exist in most particle impact experiments, and their potentially profound influence on the observed behavior must be considered when interpreting experimental results at a quantitative level. This is particularly important because the main route to determining particle concentration from impact measurements has consisted in measuring the impact rate and inferring the concentration via modeling.

We have concentrated here on the transport of particles to an electrode via the three primary, inevitable modes of mass transport in conventional electrochemistry. Additional mechanisms can profoundly influence transport, however, for example dielectrophoresis and electrothermal fluid flows induced by a purposefully applied AC excitation [29, 30], self-propelled biocatalytic micromotors [31], active pumping via on-chip electrodes in microfluidics [32], dynamic chemical interactions with the electrode [33], and various forms of confinement [34]. An area that was not addressed systematically in the primary literature so far is the influence of migration and convection on the distribution of landing sites of particles on an electrode, which has important consequences for interpreting current blockade experiments or when using impact methods for assembling advanced materials [35]. Both diffusion and migration lead to uneven particle distributions for all but the simplest geometries. For example, particles tend to accumulate near the edges of shrouded disk electrodes [36, 37]. Several approaches have been introduced recently to mitigate these effects include the use of hemispherical [14] and ring [37] electrodes as well as electrocatalytic interruption [38]. Finally, we have not addressed here the information that can be extracted from the shape of the transients during impact events, a promising route for extracting quantitative information from impact measurements [15, 39].

We also discussed the forces generated when a particle is tethered to an electrode at which a faradaic reaction takes place. To date much of the focus of impact electrochemistry has been on the development and understanding of the methods themselves. As the field matures, however, one can expect the focus to shift increasingly towards their utilization as readout modality in more complex experiments, where tethered constructs may prove essential.

Acknowledgment

SGL thanks the great educator Alexander Y. Grosberg for an insightful discussion on electrophoresis many years ago. JED thanks the National Science Foundation Chemical Measurement and Imaging Program (grant CHE-2003587) for funding.

Annotated references

[3] *
Arguably the first explicit experimental demonstration of particle impact electrochemistry and emphasizing the role of migration.

[24] **
Experimental demonstration and theoretical analysis of the role of self-induced convection in impact electrochemistry.

[25] **
Experimental demonstration and theoretical analysis of the role of self-induced convection in impact electrochemistry.

[36] *
Dramatic illustration of the importance of migration in particle impact experiments.

[38] *
Creative concept to manipulate mediator mass transport in the vicinity of an electrode and thus mitigate experimental biases.

Declaration of interest

None.

References

[1] Baker LA. Perspective and Prospectus on Single-Entity Electrochemistry. J Am Chem Soc. 2018;140:15549-59.
[2] Lemay SG, Moazzenzade T. Single-Entity Electrochemistry for Digital Biosensing at Ultralow Concentrations. Anal Chem. 2021;93:9023-31.
[3] Quinn BM, van 't Hof P, Lemay SG. Time-resolved electrochemical detection of discrete adsorption events. J Am Chem Soc. 2004;126:8360-1.
[4] Deng Z, Renault C. Detection of individual insulating entities by electrochemical blocking. Current Opinion in Electrochemistry. 2021;25:100619.
[5] Zhou Y-G, Rees NV, Compton RG. The Electrochemical Detection and Characterization of Silver Nanoparticles in Aqueous Solution. Angewandte Chemie International Edition. 2011;50:4219-21.
[6] Xiao X, Bard AJ. Observing single nanoparticle collisions at an ultramicroelectrode by electrocatalytic amplification. J Am Chem Soc. 2007;129:9610-+.
[7] Bard AJ, Faulkner LR. Electrochemical Methods: Fundamentals and Applications. New York: John Wiley & Sons; 2001.
[8] Eloul S, Kätelhön E, Compton RG. When does near-wall hindered diffusion influence mass transport towards targets? Phys Chem Chem Phys. 2016;18:26539-49.
[9] Lyklema J. Fundamentals of Interface and Colloid Science, Vol II: Solid-Liquid Interfaces. San Diego: Academic Press; 1995.
[10] Ahmed JU, Lutkenhaus JA, Alam MS, Marshall I, Paul DK, Alvarez JC. Dynamics of Collisions and Adsorption in the Stochastic Electrochemistry of Emulsion Microdroplets. Anal Chem. 2021;93:7993-8001.
[11] Oldham KB. Theory of microelectrode voltammetry with little electrolyte. J Electroanal Chem Interfacial Electrochem. 1988;250:1-21.
[12] Renault C, Lemay SG. Electrochemical Collisions of Individual Graphene Oxide Sheets: An Analytical and Fundamental Study. ChemElectroChem. 2020;7:69-73.
[13] Goines S, Dick JE. Review—Electrochemistry's Potential to Reach the Ultimate Sensitivity in Measurement Science. Journal of The Electrochemical Society. 2020;167:037505.
[14] Deng Z, Elattar R, Maroun F, Renault C. In Situ Measurement of the Size Distribution and Concentration of Insulating Particles by Electrochemical Collision on Hemispherical Ultramicroelectrodes. Anal Chem. 2018;90:12923-9.
[15] Ahmed JU, Lutkenhaus JA, Tubbs A, Nag A, Christopher J, Alvarez JC. Estimating Average Velocities of Particle Arrival Using the Time Duration of the Current Signal in Stochastic Blocking Electrochemistry. Anal Chem. 2022.
[16] Jackson JD. Classical Electrodynamics, 2nd edition. New York: John Wiley & Sons; 1975.
[17] Oja SM, Robinson DA, Vitti NJ, Edwards MA, Liu Y, White HS, et al. Observation of Multipeak Collision Behavior during the Electro-Oxidation of Single Ag Nanoparticles. J Am Chem Soc. 2017;139:708-18.
[18] Robinson DA, Liu Y, Edwards MA, Vitti NJ, Oja SM, Zhang B, et al. Collision Dynamics during the Electrooxidation of Individual Silver Nanoparticles. J Am Chem Soc. 2017;139:16923-31.
[19] Ma W, Ma H, Chen J-F, Peng Y-Y, Yang Z-Y, Wang H-F, et al. Tracking motion trajectories of individual nanoparticles using time-resolved current traces. Chemical Science. 2017;8:1854-61.
[20] Ustarroz J, Kang M, Bullions E, Unwin PR. Impact and oxidation of single silver nanoparticles at electrode surfaces: one shot versus multiple events. Chemical Science. 2017;8:1841-53.

[21] Patel AN, Martinez-Marrades A, Brasiliense V, Koshelev D, Besbes M, Kuszelewicz R, et al. Deciphering the Elementary Steps of Transport-Reaction Processes at Individual Ag Nanoparticles by 3D Superlocalization Microscopy. Nano Lett. 2015;15:6454-63.
[22] Kline TR, Paxton WF, Wang Y, Velegol D, Mallouk TE, Sen A. Catalytic micropumps: Microscopic convective fluid flow and pattern formation. J Am Chem Soc. 2005;127:17150-1.
[23] Branagan SP, Contento NM, Bohn PW. Enhanced Mass Transport of Electroactive Species to Annular Nanoband Electrodes Embedded in Nanocapillary Array Membranes. J Am Chem Soc. 2012;134:8617-24.
[24] Thorgaard SN, Jenkins S, Tarach AR. Influence of Electroosmotic Flow on Stochastic Collisions at Ultramicroelectrodes. Anal Chem. 2020;92:12663-9.
[25] Moazzenzade T, Yang X, Walterbos L, Huskens J, Renault C, Lemay SG. Self-Induced Convection at Microelectrodes via Electroosmosis and Its Influence on Impact Electrochemistry. J Am Chem Soc. 2020;142:17908-12.
[26] Pendergast AD, Deng Z, Maroun F, Renault C, Dick JE. Revealing Dynamic Rotation of Single Graphene Nanoplatelets on Electrified Microinterfaces. ACS Nano. 2021;15:1250-8.
[27] Long D, Viovy JL, Ajdari A. Stretching DNA with electric fields revisited. Biopolymers. 1996;39:755-9.
[28] van Dorp S, Keyser UF, Dekker NH, Dekker C, Lemay SG. Origin of the electrophoretic force on DNA in solid-state nanopores. Nature Physics. 2009;5:347-51.
[29] Frkonja-Kuczin A, Ray L, Zhao Z, Konopka MC, Boika A. Electrokinetic preconcentration and electrochemical detection of Escherichia coli at a microelectrode. Electrochimica Acta. 2018;280:191-6.
[30] Bonezzi J, Luitel T, Boika A. Electrokinetic Manipulation of Silver and Platinum Nanoparticles and Their Stochastic Electrochemical Detection. Anal Chem. 2017;89:8614-9.
[31] Guo Z, Wu Y, Xie Z, Shao J, Liu. J, Yao Y, et al. Self-Propelled Initiative Collision at Microelectrodes with Vertically Mobile Micromotors. Angewandte Chemie International Edition. 2022;61:e202209747.
[32] Weiß LJK, Music E, Rinklin P, Banzet M, Mayer D, Wolfrum B. On-Chip Electrokinetic Micropumping for Nanoparticle Impact Electrochemistry. Anal Chem. 2022;94:11600-9.
[33] Lu S-M, Li M-Y, Long Y-T. Dynamic Chemistry Interactions: Controlled Single-Entity Electrochemistry. The Journal of Physical Chemistry Letters. 2022;13:4653-9.
[34] Jaugstetter M, Blanc N, Kratz M, Tschulik K. Electrochemistry under confinement. Chem Soc Rev. 2022;51:2491-543.
[35] Oladeji AV, Courtney JM, Fernandez-Villamarin M, Rees NV. Electrochemical Metal Recycling: Recovery of Palladium from Solution and In Situ Fabrication of Palladium-Carbon Catalysts via Impact Electrochemistry. J Am Chem Soc. 2022;144:18562-74.
[36] Fosdick SE, Anderson MJ, Nettleton EG, Crooks RM. Correlated Electrochemical and Optical Tracking of Discrete Collision Events. J Am Chem Soc. 2013;135:5994-7.
[37] Moazzenzade T, Walstra T, Yang X, Huskens J, Lemay SG. Ring Ultramicroelectrodes for Current-Blockade Particle-Impact Electrochemistry. Anal Chem. 2022.
[38] Chung J, Hertler P, Plaxco KW, Sepunaru L. Catalytic Interruption Mitigates Edge Effects in the Characterization of Heterogeneous, Insulating Nanoparticles. J Am Chem Soc. 2021;143:18888-98.
[39] Chung HJ, Lee J, Hwang J, Seol KH, Kim KM, Song J, et al. Stochastic Particle Approach Electrochemistry (SPAE): Estimating Size, Drift Velocity, and Electric Force of Insulating Particles. Anal Chem. 2020;92:12226-34.